



HAL
open science

Variability in growth and tissue composition (CNP, natural isotopes) of the three morphotypes of holopelagic *Sargassum*

T. Changeux, L. Berline, W. Podlejski, T. Guillot, V. Stiger-Pouvreau, S. Connan, T. Thibaut

► To cite this version:

T. Changeux, L. Berline, W. Podlejski, T. Guillot, V. Stiger-Pouvreau, et al.. Variability in growth and tissue composition (CNP, natural isotopes) of the three morphotypes of holopelagic *Sargassum*. *Aquatic Botany*, 2023, 187, pp.103644. 10.1016/j.aquabot.2023.103644 . hal-04229865v2

HAL Id: hal-04229865

<https://hal.science/hal-04229865v2>

Submitted on 5 Oct 2023

HAL is a multi-disciplinary open access archive for the deposit and dissemination of scientific research documents, whether they are published or not. The documents may come from teaching and research institutions in France or abroad, or from public or private research centers.

L'archive ouverte pluridisciplinaire **HAL**, est destinée au dépôt et à la diffusion de documents scientifiques de niveau recherche, publiés ou non, émanant des établissements d'enseignement et de recherche français ou étrangers, des laboratoires publics ou privés.

Title.

Variability in growth and tissue composition (CNP, natural isotopes) of the three morphotypes of holopelagic *Sargassum*

Authors names and affiliations.

Changeux T. (ORCID 0000-0002-0418-3321); e-mail: thomas.changeux@ird.fr; Affiliation: Mediterranean institute of oceanography (MIO); Postal address: Institut Méditerranéen d'Océanologie (MIO) - Equipe 5 EMBIO, Campus de Luminy, Case 901, Océanomed, Bât. Méditerranée 26M/102, 13288 Marseille Cédex 9

Berline L. (ORCID 0000-0002-5831-7399); e-mail: leo.berline@mio.osupytheas.fr; Affiliation: MIO

Podlejski W. (ORCID 0000-0002-3286-4984), e-mail: witold.podlejski@mio.osupytheas.fr; Affiliation: MIO

Guillot T., e-mail: tymguillot@gmail.com; Affiliation: Ifremer Martinique, 79 route de Pointe Fort 97231 Le Robert

Stiger-Pouvreau V. (ORCID 0000-0003-3041-0468), e-mail: valerie.stiger@univ-brest.fr; Affiliation: Univ Brest, CNRS, IRD, Ifremer, LEMAR, F-29280. Plouzane, France

Connan S. (ORCID 0000-0002-8280-1041), e-mail: solene.connan@univ-brest.fr; Affiliation: Univ Brest, CNRS, IRD, Ifremer, LEMAR, F-29280. Plouzane, France

Thibaut T. (ORCID 0000-0001-8530-9266); e-mail: thierry.thibaut@univ-amu.fr; Affiliation: MIO

Corresponding author

Changeux T. e-mail : thomas.changeux@ird.fr; Affiliation: MIO

Highlights

- *Sargassum fluitans* III growth rate is the highest.
- *Sargassum natans* I growth rate is the lowest.
- Tissue composition differs between morphotypes.

Abstract

Holopelagic *Sargassum* blooms in the tropical North Atlantic since 2011 are composed of two species, *Sargassum natans* and *S. fluitans*, and three morphotypes: *S. natans* VIII, *S. natans* I and *S. fluitans* III. The distinct morphology and the variations in space and time of the proportion of these three morphotypes suggest that they may have different physiology. For the first time, we have quantified the growth rates of these three morphotypes through *in situ* 9-day experiments on the coast of Martinique Island (French West Indies). Despite the non-optimal conditions for growth for these pelagic species and the short time of the experiment, we have observed that *Sargassum fluitans* III was growing faster (approximately twice as fast) than *S. natans* VIII and *S. natans* I. *Sargassum natans* I exhibited the slowest growth. The differences in tissue composition (CNP and CN natural isotopes) of morphotypes point to a greater benefit for *S. fluitans* III from the coastal localization of our experiment than for the two *S. natans* morphotypes, and suggest that *S. natans* I had achieved its last growth further offshore before our experiment. These contrasting growth performances are consistent with the dominance of *S. fluitans* III in recent observations in the Caribbean region and along the path from the *Sargassum* belt. This also makes this last morphotype the best candidate for cultivation. Making the distinction between the growth performances of morphotypes may improve the current predictive models about dispersal of these species.

Keywords

Seaweed, Brown macroalgae, Sargasso, Carbon, Nitrogen, Phosphorus, Algal bloom, *In-situ* culture.

1 1. Introduction

2 Since 2011, the tropical North Atlantic Ocean has been the site of seasonal blooms of holopelagic
3 *Sargassum*, rooted in the North Equatorial Recirculation Region. Holopelagic *Sargassum* are currently
4 forming the Great Atlantic *Sargassum* Belt that can be observed from space (Wang et al., 2019), and
5 causes strandings westwards, along the whole of the North Atlantic coast of South America and the
6 Caribbean area, including the Gulf of Mexico, and eastwards along the West African coasts (Berline et
7 al., 2020).

8 These strandings are composed of three distinct morphotypes: *Sargassum natans* VIII Parr, *S.*
9 *natans* I Parr, and *S. fluitans* III Parr (Schell et al., 2015). Each morphotype shows a distinct
10 morphology especially blade size, number of blades and air bladders (floats) per stem, and presence
11 of thorns on the stem (García-Sánchez et al., 2020; Schell et al., 2015) suggesting that the three
12 morphotypes may have different biological characteristics. This is confirmed by the recent growth
13 rates observed *in-situ* and *ex-situ* for *S. natans* VIII and *S. fluitans* III (Magaña-Gallegos et al., 2023a),
14 and *ex-situ* for the three morphotypes (Magaña-Gallegos et al., 2023b).

15 Since the beginning of *Sargassum* blooms in 2011, significant variations of the abundance in
16 morphotype composition have been observed. Initially, *S. natans* VIII was dominant in the south
17 (Antilles Current, Eastern Caribbean and Western Tropical Atlantic) and *S. natans* I in the north (south
18 of the Sargasso Sea) (Schell et al., 2015; November 2014 to May 2015). In 2017, during two open
19 ocean campaigns along a latitudinal gradient from Guyana to the Sargasso Sea
20 (<https://doi.org/10.17600/17004300>) in May/June and following a longitudinal transatlantic route
21 (<https://doi.org/10.17600/17016900>) in October from Cabo Verde Island to Guadeloupe, *S. fluitans*
22 III appeared to be dominant north of Guadeloupe for the first cruise and everywhere for the second
23 cruise. More recently, studies have shown a quasi-permanent dominance of *S. fluitans* III in
24 *Sargassum* strandings on Mexican Caribbean shores from 2016 to 2020 (Vázquez-Delfín et al., 2021;
25 García-Sánchez et al., 2020), along the Jamaican coast (Machado et al., 2022), and on the Caribbean,

26 Florida and Bahamas coasts (Iporac et al., 2022) as well as on a transatlantic cruise in 2022
27 (<https://energieaugrandlarg.wixsite.com/website>).

28 Biological models of *Sargassum* dynamics in the Atlantic Ocean (Brooks et al., 2018; Jouanno et al.,
29 2021) use parameters based on physiological studies that do not differentiate between morphotypes
30 (Hanisak and Samuel, 1987; Lapointe, 1995; Lapointe et al., 2014). However in macroalgae, the life
31 traits are often taxon-dependent (Vranken et al., 2022) and therefore could explain the variations in
32 dominance between morphotypes with time and across the North Atlantic Ocean. Taking into
33 account differential growth rate may improve the model simulations.

34 Differential physiology would also impact tissue composition of *Sargassum* in CNP including C:N, N:P,
35 C:P ratios and $\delta^{13}\text{C}$, $\delta^{15}\text{N}$ isotopes, as it integrates *Sargassum* environmental history along its drift
36 path (Lapointe et al., 2021; Vázquez-Delfín et al., 2021).

37 The aim of this work was then to quantify the growth rates and tissue CNP composition of the three
38 morphotypes through *in situ* short term experiments in Martinique Island (French West Indies).

39 **1 Materials and methods**

40 **1.1 Location of experimental site and *Sargassum* sampling**

41 Experiments were performed on the east coast of Martinique Island, in Baie du Robert, close to the
42 Ifremer marine station, where a meteorological station is located. It took place in May-June 2021,
43 when the Island is frequently supplied with *Sargassum* (Johns et al., 2020). This shallow bay (<30 m
44 depth) faces the Atlantic Ocean and receives *Sargassum* pushed by the northeast trade winds after
45 passing over the continental shelf, which extends for more than 15 km offshore (Fig. S1).

46 The nutrient concentrations (NO_3^- , NO_2^- , NH_4^+ , PO_4^{2-}) of surface seawater in the bay was monitored
47 once every 2 months since 2017 as part of an extension of Ifremer's REPHY network (Belin et al.,
48 2021) to the French overseas territories. The values (mean \pm SD) measured at the REPHY station,
49 situated 400 m from our experimental site (S1), were low for a coastal station, especially when

50 considering the different forms of N, $\text{NO}_3^- + \text{NO}_2^-$ ($0.3 \pm 0.3 \mu\text{mol/L}$) and NH_4^+ ($0.3 \pm 0.3 \mu\text{mole/L}$), with
51 regard to PO_4^{2-} ($0.07 \pm 0.05 \mu\text{mol/L}$). This absence of pollution is confirmed by a previous detailed
52 study of the bay (De Rock et al., 2019).

53 1.2 *Growth experiment*

54 *Sargassum* individuals were collected off the coast within the bay selecting the young clumps
55 following the criteria of Stoner and Greening (1984) to age the clumps. For each morphotype, we cut
56 fragments of 5 to 20 cm length from the apical part, free from visible epiphytes. To be consistent
57 with field observations, the three morphotypes were grown together. Approximately 20 g of wet
58 weight of each morphotype (5-10 fragments, 60 g in total) hereinafter called a batch, were placed in
59 5 L transparent plastic bottles, perforated with one hundred holes to allow good water circulation
60 (see Fig. S2 showing cultivation device). The density of 60 g for 5 L was chosen after trials to increase
61 the time before first signs of degradation while maintaining a sufficient quantity of *Sargassum* for the
62 analyses. These bottles were attached to mooring cables at 2 m depth to avoid destruction of the
63 devices by wave effect. Temperature and light inside two of the four bottles was recorded with UA-
64 002-08 (HOBO) data loggers.

65 The entire experiment lasted 9 days, from May 25th to June 3rd 2021. The wet weight was measured
66 every 3 days both for batches and individuals. The wet weight of each batch was measured on a
67 BAXTRAN BR balance (0.1 g readability) after dewatering using absorbent paper in a salad spinner.
68 Inside each batch, three individuals per morphotype ($n = 36$) were identified with colored beads
69 strung on a nylon thread attached to the fragment. The wet weight of each individual ($n = 12$ per
70 morphotype) was obtained as for the batch but by using a more accurate balance (PRECISA 321LT,
71 0.1 mg readability). In addition, the number of floats was counted for each individual.

72 1.3 *Water, tissue, and data analysis*

73 At the beginning of the experiment, and before each measurement session, we sampled the water in
74 200 mL plastic bottles to measure nutrient composition. The sample was fixed with 100 μL HgCl_2 per

75 bottle, and then stored in a cool place protected from light. The analyses were carried out by
76 automated colorimetry for NO_3^- , NO_2^- , NH_4^+ , PO_4^{2-} (Aminot and K  rouel, 2007) and for NH_4^+ (Holmes
77 et al., 1999).

78 At the end of the experiment, eight samples (mix of individuals) of 5 g wet weight of each
79 morphotype were analyzed for C, N, P, $\delta^{13}\text{C}$ and $\delta^{15}\text{N}$ tissue composition. These samples were dried
80 in an oven at 60  C during 48 h, reduced into powder, acidified to eliminate mineral sources of
81 carbon, and analyzed by spectrometry following Raimbault et al. (2008).

82 The growth rate (GR) in weight was calculated in d^{-1} following:

$$GR_d = \frac{1}{d} \ln \left(\frac{W_d}{W_0} \right)$$

83 were d = number of days ($d = 9$ for the entire experiment) and W_d = wet weight at day d , W_0 = wet
84 weight at day 0.

85 The floats ratio (FR) was calculated (in %) with reference to the initial number of floats for the entire
86 experiment following:

$$FR = \frac{N_9}{N_0} \cdot 100$$

87 were N_9 = number of floats at day 9 and N_0 = number of floats at day 0.

88 Non parametric Kruskal-Wallis test (KW test) followed by Dunns post-hoc test were used to test the
89 morphotype effect on *Sargassum* GR, FR and tissue composition with a significance level of 0.05.

90 **2 Results**

91 *2.1 Field conditions*

92 During the 9 days of experiment, water temperature inside the bottles varied from 28  C at night to
93 31  C during the day (06:00 AM-6:00 PM) when light inside the bottle varied from 74 to
94 740 $\mu\text{mol photons m}^{-2} \text{ s}^{-1}$ with a mean value of 137 $\mu\text{mol photons m}^{-2} \text{ s}^{-1}$. The nutrient concentrations

95 were high and variable compared to REPHY measurements (respectively 1.7 ± 2.0 vs 0.3 ± 0.3 $\mu\text{mol/L}$
96 for $\text{NO}_3^- + \text{NO}_2^-$, 2.1 ± 1.7 vs 0.3 ± 0.3 $\mu\text{mol/L}$ for NH_4^+ and 0.3 ± 0.3 vs 0.07 ± 0.05 $\mu\text{mol/L}$ for PO_4^{2-}).
97 The daily rainfall, including one day before the start of the experiment, varied from 0 to 10.6 mm,
98 with a mean of 1.52 mm which is below the average of 2.07 mm from May to June 2021 at the
99 station. The wind speed and direction were regular for the season ($9.73 \text{ m}\cdot\text{s}^{-1}$ oriented WNW
100 (67.27°)). The high nutrient values compared to REPHY station were mainly related to the location of
101 our experimental site closer to the coast and human activities.

102 2.2 *Patterns of change in the Sargassum weight and floats ratio*

103 The increase in *Sargassum* weight along the experiment was clearly visible when considering the
104 batches (Fig. S3). After 9 days, the initial 20 g were exceeded by all morphotypes, reaching about 25 g
105 for *S. natans* VIII and *S. natans* I and approaching 30 g for *S. fluitans* III (see pictures Fig. S4). After 6
106 days, the weight increase slowed down for all morphotypes. In contrast, this increase was lower and
107 more variable in the individual measurements (Fig. S3). The floats ratio (FR) after 9 days was overall
108 below 100%, showing a loss of floats for all morphotypes (Fig. S5). This was especially the case for *S.*
109 *natans* I.

110 2.3 *Growth rate*

111 For all morphotypes, the GR over every 3-day period decreased overall over time from the beginning
112 of the experiment (Fig. 1 A). The median value of batch GR varied from 0.063 to 0.022 d^{-1} after 3
113 days, from 0.044 to 0.018 d^{-1} after 6 days, and from 0.019 to -0.006 d^{-1} after 9 days.
114 *Sargassum fluitans* III had always the highest GR values and *S. natans* I the lowest. *Sargassum natans*
115 VIII GR was intermediate. After 9 days, the individual GR showed a significant variation between
116 morphotypes (KW test $\chi^2 = 16.244$, $\text{df} = 2$, $p\text{-value} = 0.0002969$). The Dunns post hoc test gives two
117 significant results: *S. fluitans* III vs *S. natans* I ($p=0.0000678^{***}$) and *S. fluitans* III vs *S. natans* VIII
118 ($p=0.0313^*$). Even if the mean individual GR of *S. natans* I was negative, linked with the first signs of
119 senescence, the mean batch GR of this morphotype was positive (Fig. 1 B).

120 2.4 Tissue elemental composition (C, N, P, $\delta^{13}\text{C}$, $\delta^{15}\text{N}$) of *Sargassum*

121 The effect of morphotype was significant only for %N, $\delta^{15}\text{N}$, $\delta^{13}\text{C}$ and C:N (Table S1). For other
122 elements, the median values were %C = 23.52%, %P = 0.07%, N:P = 30.33 and C:P = 827.43.

123 The post hoc Dunn tests (Fig. 2; Table S1) showed that *S. fluitans* III was characterized by a high %N,
124 $\delta^{15}\text{N}$ and low C:N and $\delta^{13}\text{C}$. In contrast, *S. natans* VIII showed low %N, $\delta^{15}\text{N}$ and high C:N and $\delta^{13}\text{C}$ and
125 *S. natans* I was essentially characterized by a low $\delta^{15}\text{N}$.

126 3 Discussion

127 3.1 Changes in growth performance during the experiment

128 For the three morphotypes, GR (0.02-0.04 d⁻¹ for batches) were in the low range of literature growth
129 data reported by Brooks et al. (2018), *i.e.* [0.029-0.11] d⁻¹ relying on *in situ* (Lapointe, 1986; Lapointe
130 et al., 2014) and laboratory experiments (Hanisak and Samuel, 1987). In addition, GR decreased with
131 time for all morphotypes. This does not align with the neritic origin of our samples, generally
132 associated with low nutrient limitation and high GR following Lapointe (1995). These results, for both
133 batches and individuals, indicate that algae were not in optimal growth conditions. This decrease of
134 GR may be due:

- 135 - to excessively high seawater temperatures [28-31°C] observed during the experiment, as
136 decrease in growth after 24°C was observed by Hanisak and Samuel (1987) for *S. natans*;
- 137 - to light limitation since our mean light measurement of 137 $\mu\text{mol photons m}^{-2} \text{s}^{-1}$ in the bottle
138 corresponds to intermediate GR of 0.02 d⁻¹ (Hanisak and Samuel, 1987);
- 139 - to stress related to the confinement in the bottles despite the numerous holes made in order
140 to renew the water. On the one hand, pelagic *Sargassum* are known to produce large
141 quantities of dissolved organic carbon (Powers et al., 2019) that promote, together with high
142 nutrient level, bacterial growth (Michotey et al., 2020). On the other hand, the lack of
143 ventilation may lead to micronutrient depletion.

144 GR did not correspond to maximum growth values, taking into account both the phenomenon of
145 growth and senescence over 9 days. Although culture conditions may be limiting, our results clearly
146 show contrasting performances among morphotypes.

147 3.2 *Differential growth between the 3 morphotypes and implications*

148 *Sargassum fluitans* III was growing faster, approximately twice as fast as *S. natans* VIII and *S. natans* I.
149 This is consistent with lab experiment results of Hanisak and Samuel (1987), and *ex-situ* experiments
150 of Magaña-Gallegos et al. (2023b), but differs from *ex-situ* and *in-situ* experiments for only two
151 morphotypes of Magaña-Gallegos et al. (2023a). Moreover, *S. natans* I exhibited the slowest growth
152 rate. This suggests that growth is morphotype dependent. When exposed to high temperature, high
153 nutrient concentration and a slight light limitation, *S. fluitans* III does better than *S. natans* I.

154 These differences may have implications with regard to the relative abundance of morphotypes
155 observed at sea and in strandings. However GR cannot be simply translated into abundances. The
156 coexistence of the three morphotypes suggests that processes other than growth maintain
157 competitive success of the *S. natans* morphotypes despite lower GR. Morphotypes may have
158 differing environmental niches that were not spanned by our experimental conditions. For instance,
159 in a more oligotrophic and colder environment than ours, *S. natans* I dominated during 2014 and
160 2015 north of 24°N (Schell et al., 2015). Magaña-Gallegos et al. (2023b) also found that morphotypes
161 had distinct temperature optima.

162 Future measurements of growth in contrasted conditions may help to explain field observations of
163 morphotype composition and the dominance of *S. fluitans* III in the Caribbean region and along the
164 path from the *Sargassum* belt.

165 3.3 *Significance of CNP and isotope composition*

166 Our results showed significant differences of %N, $\delta^{15}\text{N}$, $\delta^{13}\text{C}$ and C:N between morphotypes while no
167 difference has been found between *S. natans* and *S. fluitans* in the large (n = 488) and long-term

168 dataset of Lapointe et al. (2021). Even if the tissue composition prior to experiment is unknown this
169 discrepancy can be explained by the particular environmental history of our samples.

170 Overall, %N and %P cannot explain the different GR among morphotypes. Both *S. fluitans* III and *S.*
171 *natans* I have similar %N and %P values, but different GR. It may be related to nutrient uptake that
172 occurred before the experiment. To improve interpretations, future experiments should include
173 isotopes analyses on freshly arrived *Sargassum* before starting the experiment.

174 The high N:P (30.33) and C:P value (827) of all morphotypes in our experiment suggests a limitation
175 in P, as pointed out by Lapointe et al. (2021) for samples collected after 2010s. This P limitation may
176 explain why %N differences do not result in growth rate variations.

177 The value of %C (23.5%) was low compared to the recent Mexican samples of Vázquez-Delfín et al.
178 (2021). Conversely, %N values were high in agreement with the Lapointe et al. (2021) data for the
179 2010s, except for *S. natans* VIII which were lower in our study. The high C:N values (36) of *S. natans*
180 VIII suggest that this morphotype was not in good growing conditions.

181 The isotopic composition showed high values in $\delta^{13}\text{C}$ which are footprints of the continental origin of
182 C as a consequence of the coastal situation of our samples. The low values of $\delta^{15}\text{N}$ of *S. natans* I may
183 be indicative of diazotrophic fixation, common in pelagic *Sargassum* (Carpenter, 1972; Phlips and
184 Zeman, 1990) while higher values may indicate enrichment by NO_3^- present along the coast (Lapointe
185 et al., 2021; Montoya, 2008). It is interesting to note that $\delta^{15}\text{N}$ order among morphotypes follow the
186 GR. This suggests that higher $\delta^{15}\text{N}$ indicate more recent growth fueled by coastal NO_3^- . That implies
187 that the last growth of *S. natans* I was achieved at a greater distance in time and offshore. However,
188 we would need the composition before the experiment to conclude with certainty on this point.

189 Thus, the significant variations of the elemental composition point to a greater benefit for *S. fluitans*
190 III from the coastal situation of our experiment than for the two *S. natans* morphotypes.

191 In conclusion, despite the non optimal conditions encountered in this *in situ* experiment, it shows for
192 the first time contrasting growth performances between the three morphotypes that are consistent

193 with their abundance in the field. Current models including algal growth, which do not distinguish
194 between morphotypes, can be improved by taking these morphotype growth differences into
195 account. These differences in growth are probably linked to photosynthetic processes between
196 morphotypes that will have to be specified with new experiments. *Sargassum fluitans* III appears
197 here as the most tolerant morphotype, best candidate for nearshore and indoor cultivation.

198 **4 Funding**

199 This research was supported by the French Agence Nationale de la Recherche Sargassum grants
200 FORESEA (ANR-19-SARG-0007-01) and SAVE-C (ANR-19-SARG-0008) and by the French Institut de
201 Recherche pour le Développement Long-term Mission funding.

202 **5 Credit authorship contribution statement**

203 Conceptualization, Data curation, Methodology, Software, Supervision, Validation, Visualization (TC,
204 LB), Formal analysis (TC, LB, WP), Funding acquisition, Project administration, Resources (TC, LB, TT),
205 Investigation (TC, TG), Writing (TC, LB, SC, VSP, TT).

206 **6 Declaration of Competing Interest**

207 None

208 **7 Acknowledgements**

209 We are grateful to Emmanuel Thouard, Ifremer Martinique, who gave access to Ifremer station
210 facilities and meteorological data, Jean-Pierre Allenou, Ifremer Martinique, for the REPHY data and
211 Samson Devillers, Ifremer Martinique, for his operational assistance. Tissue analysis was performed
212 by PACEM Mediterranean Institute of Oceanography (MIO) intern platform. Patrick Raimbault, from
213 the MIO, helped with interpretation. The map in Fig. S1 was partly produced by Felix Navarro MIO
214 internship from AgroParisTech.

215 **8** References

- 216 Aminot, A., K erouel, R., 2007. Dosage automatique des nutriments dans les eaux marines: m ethodes
217 en flux continu. Ifremer, France.
- 218 Belin, C., Soudant, D., Amzil, Z., 2021. Three decades of data on phytoplankton and phycotoxins on
219 the French coast: Lessons from REPHY and REPHYTOX. Harmful Algae 102, 101733.
220 <https://doi.org/10.1016/j.hal.2019.101733>
- 221 Berline, L., Ody, A., Jouanno, J., Chevalier, C., Andr e, J.-M., Thibaut, T., M enard, F., 2020. Hindcasting
222 the 2017 dispersal of *Sargassum* algae in the Tropical North Atlantic. Marine Pollution
223 Bulletin 158, 111431. <https://doi.org/10.1016/j.marpolbul.2020.111431>
- 224 Brooks, M., Coles, V., Hood, R., Gower, J., 2018. Factors controlling the seasonal distribution of
225 pelagic *Sargassum*. Mar. Ecol. Prog. Ser. 599, 1–18. <https://doi.org/10.3354/meps12646>
- 226 Brooks, M.T., Coles, V.J., Coles, W.C., 2019. Inertia Influences Pelagic *Sargassum* Advection and
227 Distribution. Geophys. Res. Lett. 46, 2610–2618. <https://doi.org/10.1029/2018GL081489>
- 228 Carpenter, E.J., 1972. Nitrogen Fixation by a Blue-Green Epiphyte on Pelagic *Sargassum*. Science 178,
229 1207–1209. <https://doi.org/10.1126/science.178.4066.1207>
- 230 De Rock, P., Cimiterra, N., Allenou, J.-P., 2019. R ealisation d’un suivi du milieu marin en vue de la
231 mise en oeuvre de la nouvelle station d’ epuration (Pontal ery) au Robert - Caract erisation de
232 l’ etat initial (Rapport Ifremer). Le Robert (Martinique).
- 233 Garc ia-S anchez, M., Graham, C., Vera, E., Escalante-Mancera, E.,  lvarez-Filip, L., van Tussenbroek,
234 B.I., 2020. Temporal changes in the composition and biomass of beached pelagic *Sargassum*
235 species in the Mexican Caribbean. Aquatic Botany 167, 103275.
236 <https://doi.org/10.1016/j.aquabot.2020.103275>
- 237 Hanisak, M.D., Samuel, M.A., 1987. Growth rates in culture of several species of *Sargassum* from
238 Florida, USA, in: Ragan, M.A., Bird, C.J. (Eds.), Twelfth International Seaweed Symposium.
239 Springer Netherlands, Dordrecht, pp. 399–404. [https://doi.org/10.1007/978-94-009-4057-
240 4_59](https://doi.org/10.1007/978-94-009-4057-4_59)
- 241 Holmes, R.M., Aminot, A., K erouel, R., Hooker, B.A., Peterson, B.J., 1999. A simple and precise
242 method for measuring ammonium in marine and freshwater ecosystems. Can. J. Fish. Aquat.
243 Sci. 56, 1801–1808. <https://doi.org/10.1139/f99-128>
- 244 Iporac, L.A.R., Hatt, D.C., Bally, N.K., Castro, A., Cardet, E., Mesidor, R., Olszak, S., Duran, A.,
245 Burkholder, D.A., Collado-Vides, L., 2022. Community-based monitoring reveals
246 spatiotemporal variation of sargasso inundation levels and morphotype dominance across
247 the Caribbean and South Florida. Aquatic Botany 182, 103546.
248 <https://doi.org/10.1016/j.aquabot.2022.103546>
- 249 Johns, E.M., Lumpkin, R., Putman, N.F., Smith, R.H., Muller-Karger, F.E., T. Rueda-Roa, D., Hu, C.,
250 Wang, M., Brooks, M.T., Gramer, L.J., Werner, F.E., 2020. The establishment of a pelagic
251 *Sargassum* population in the tropical Atlantic: Biological consequences of a basin-scale long
252 distance dispersal event. Progress in Oceanography 182, 102269.
253 <https://doi.org/10.1016/j.pocean.2020.102269>
- 254 Jouanno, J., Benshila, R., Berline, L., Souli e, A., Radenac, M.-H., Morvan, G., Diaz, F., Sheinbaum, J.,
255 Chevalier, C., Thibaut, T., Changeux, T., Menard, F., Berthet, S., Aumont, O., Eth e, C., Nabat,
256 P., Mallet, M., 2021. A NEMO-based model of *Sargassum* distribution in the tropical Atlantic:
257 description of the model and sensitivity analysis (NEMO-Sarg1.0). Geosci. Model Dev. 14,
258 4069–4086. <https://doi.org/10.5194/gmd-14-4069-2021>
- 259 Lapointe, B.E., 1995. A comparison of nutrient-limited productivity in *Sargassum natans* from neritic
260 vs. oceanic waters of the western North Atlantic Ocean. Limnol. Oceanogr. 40, 625–633.
261 <https://doi.org/10.4319/lo.1995.40.3.0625>

262 Lapointe, B.E., Brewton, R.A., Herren, L.W., Wang, M., Hu, C., McGillicuddy, D.J., Lindell, S.,
263 Hernandez, F.J., Morton, P.L., 2021. Nutrient content and stoichiometry of pelagic *Sargassum*
264 reflects increasing nitrogen availability in the Atlantic Basin. *Nat Commun* 12, 3060.
265 <https://doi.org/10.1038/s41467-021-23135-7>

266 Lapointe, B.E., West, L.E., Sutton, T.T., Hu, C., 2014. Ryther revisited: nutrient excretions by fishes
267 enhance productivity of pelagic *Sargassum* in the western North Atlantic Ocean. *Journal of*
268 *Experimental Marine Biology and Ecology* 458, 46–56.
269 <https://doi.org/10.1016/j.jembe.2014.05.002>

270 Machado, C.B., Maddix, G.-M., Francis, P., Thomas, S.-L., Burton, J.-A., Langer, S., Larson, T.R., Marsh,
271 R., Webber, M., Tonon, T., 2022. Pelagic *Sargassum* events in Jamaica: Provenance,
272 morphotype abundance, and influence of sample processing on biochemical composition of
273 the biomass. *Science of The Total Environment* 817, 152761.
274 <https://doi.org/10.1016/j.scitotenv.2021.152761>

275 Magaña-Gallegos, Eden, García-Sánchez, M., Graham, C., Olivos-Ortiz, A., Siuda, A.N.S., van
276 Tussenbroek, B.I., 2023a. Growth rates of pelagic *Sargassum* species in the Mexican
277 Caribbean. *Aquatic Botany* 185, 103614. <https://doi.org/10.1016/j.aquabot.2022.103614>

278 Magaña-Gallegos, Edén, Villegas-Muñoz, E., Salas-Acosta, E.R., Barba-Santos, M.G., Silva, R., van
279 Tussenbroek, B.I., 2023b. The Effect of Temperature on the Growth of Holopelagic
280 *Sargassum* Species. *Phycology* 3, 138–146. <https://doi.org/10.3390/phycology3010009>

281 Michotey, V., Blanfuné, A., Chevalier, C., Garel, M., Diaz, F., Berline, L., Le Grand, L., Armougom, F.,
282 Guasco, S., Ruitton, S., Changeux, T., Belloni, B., Blanchot, J., Ménard, F., Thibaut, T., 2020. In
283 situ observations and modelling revealed environmental factors favouring occurrence of
284 *Vibrio* in microbiome of the pelagic *Sargassum* responsible for strandings. *Science of The*
285 *Total Environment* 748, 141216. <https://doi.org/10.1016/j.scitotenv.2020.141216>

286 Montoya, J.P., 2008. Nitrogen Stable Isotopes in Marine Environments, in: *Nitrogen in the Marine*
287 *Environment*. Elsevier, pp. 1277–1302. <https://doi.org/10.1016/B978-0-12-372522-6.00029-3>

288 Philips, E., Zeman, C., 1990. Photosynthesis, growth and nitrogen-fixation by epiphytic forms of
289 filamentous cyanobacteria from pelagic *Sargassum*. *Bulletin of Marine Science* 47(3):613-621

290 Powers, L.C., Hertkorn, N., McDonald, N., Schmitt-Kopplin, P., Del Vecchio, R., Blough, N.V., Gonsior,
291 M., 2019. *Sargassum* sp. Act as a Large Regional Source of Marine Dissolved Organic Carbon
292 and Polyphenols. *Global Biogeochem. Cycles* 33, 1423–1439.
293 <https://doi.org/10.1029/2019GB006225>

294 Raimbault, P., Garcia, N., Cerutti, F., 2008. Distribution of inorganic and organic nutrients in the South
295 Pacific Ocean – evidence for long-term accumulation of organic matter in nitrogen-depleted
296 waters. *Biogeosciences* 5, 281–298. <https://doi.org/10.5194/bg-5-281-2008>

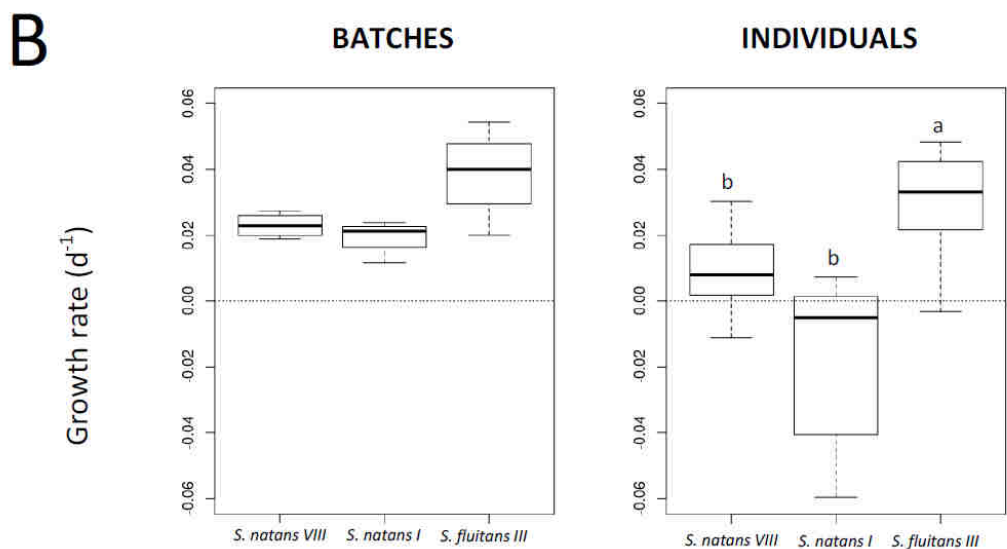
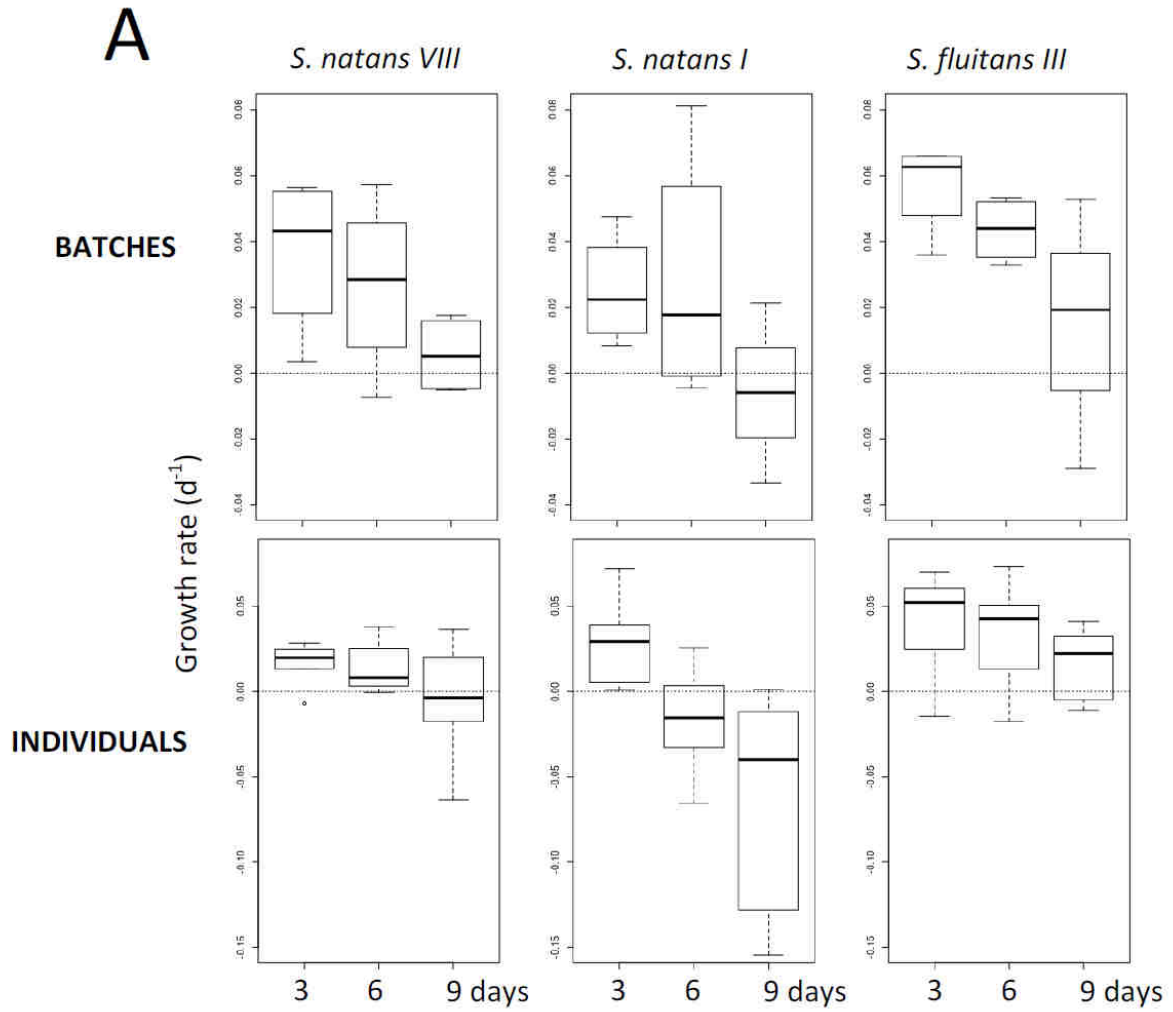
297 Schell, J., Goodwin, D., Siuda, A., 2015. Recent *Sargassum* Inundation Events in the Caribbean:
298 Shipboard Observations Reveal Dominance of a Previously Rare Form. *Oceanog* 28, 8–10.
299 <https://doi.org/10.5670/oceanog.2015.70>

300 Stoner, A., Greening, H., 1984. Geographic-variation in the macrofaunal associates of pelagic
301 *Sargassum* and some biogeographic implications. *Mar. Ecol.-Prog. Ser.* 20, 185–192.
302 <https://doi.org/10.3354/meps020185>

303 Vázquez-Delfín, E., Freile-Pelegrín, Y., Salazar-Garibay, A., Serviere-Zaragoza, E., Méndez-Rodríguez,
304 L.C., Robledo, D., 2021. Species composition and chemical characterization of *Sargassum*
305 influx at six different locations along the Mexican Caribbean coast. *Science of The Total*
306 *Environment* 795, 148852. <https://doi.org/10.1016/j.scitotenv.2021.148852>

307 Vranken, S., Robuchon, M., Dekeyzer, S., Bárbara, I., Bartsch, I., Blanfuné, A., Boudouresque, C.-F.,
308 Decock, W., Destombe, C., de Reviers, B., Díaz-Tapia, P., Herbst, A., Julliard, R., Karez, R.,
309 Kersen, P., Krueger-Hadfield, S.A., Kuhlenkamp, R., Peters, A.F., Peña, V., Piñeiro-Corbeira, C.,
310 Rindi, F., Rousseau, F., Rueness, J., Schubert, H., Sjøtun, K., Sansón, M., Smale, D., Thibaut, T.,

311 Valero, M., Vandepitte, L., Vanhoorne, B., Vergés, A., Verlaque, M., Vieira, C., Le Gall, L.,
312 Leliaert, F., De Clerck, O., 2022. AlgaeTraits: a trait database for (European) seaweeds
313 (preprint). ESSD – Ocean/Biological oceanography. <https://doi.org/10.5194/essd-2022-329>
314 Wang, M., Hu, C., Barnes, B.B., Mitchum, G., Lapointe, B., Montoya, J.P., 2019. The great Atlantic
315 *Sargassum* belt. *Science* 365, 83–87. <https://doi.org/10.1126/science.aaw7912>
316



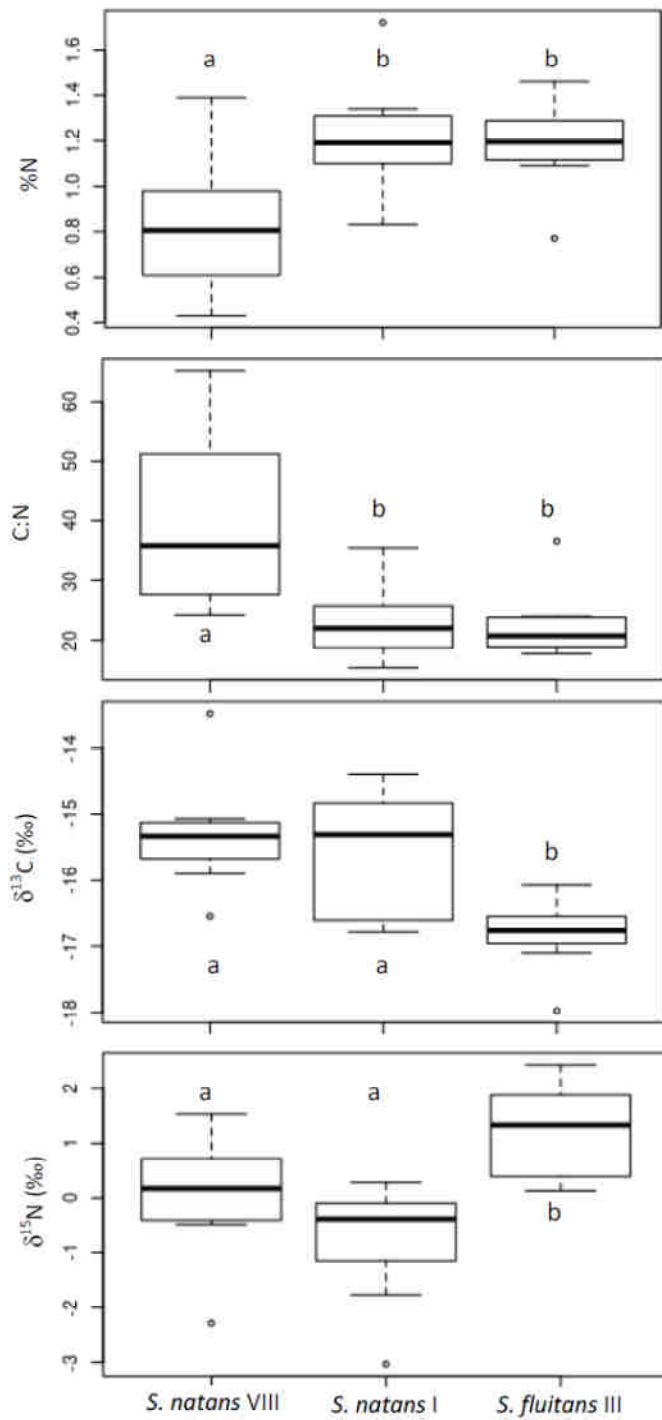
317

318 Fig. 1: Holopelagic *Sargassum* growth rate (d^{-1}) for each morphotype measured on batches ($n=4$) and
 319 individuals ($n = 12$ per morphotype) every 3 days (A.) and over the 9 days of the experiment (B.). Box
 320 shows the sample median and the first and third quartiles. Whiskers extend to the last data point

321 which is no more than 1.5 times the interquartile range. Outliers are shown as dots. The letter

322 identifies the significant differences ($p\text{-value} < 0.05$).

323



324

325 Fig. 2: Tissue composition (%N, C:N, δ¹⁵N, δ¹³C) between *Sargassum* morphotypes. Box, whiskers and

326 letters are shown as in Fig. 1.

Supplementary material of Variability in growth and tissue composition (CNP, natural isotopes) of the three morphotypes of holopelagic *Sargassum*

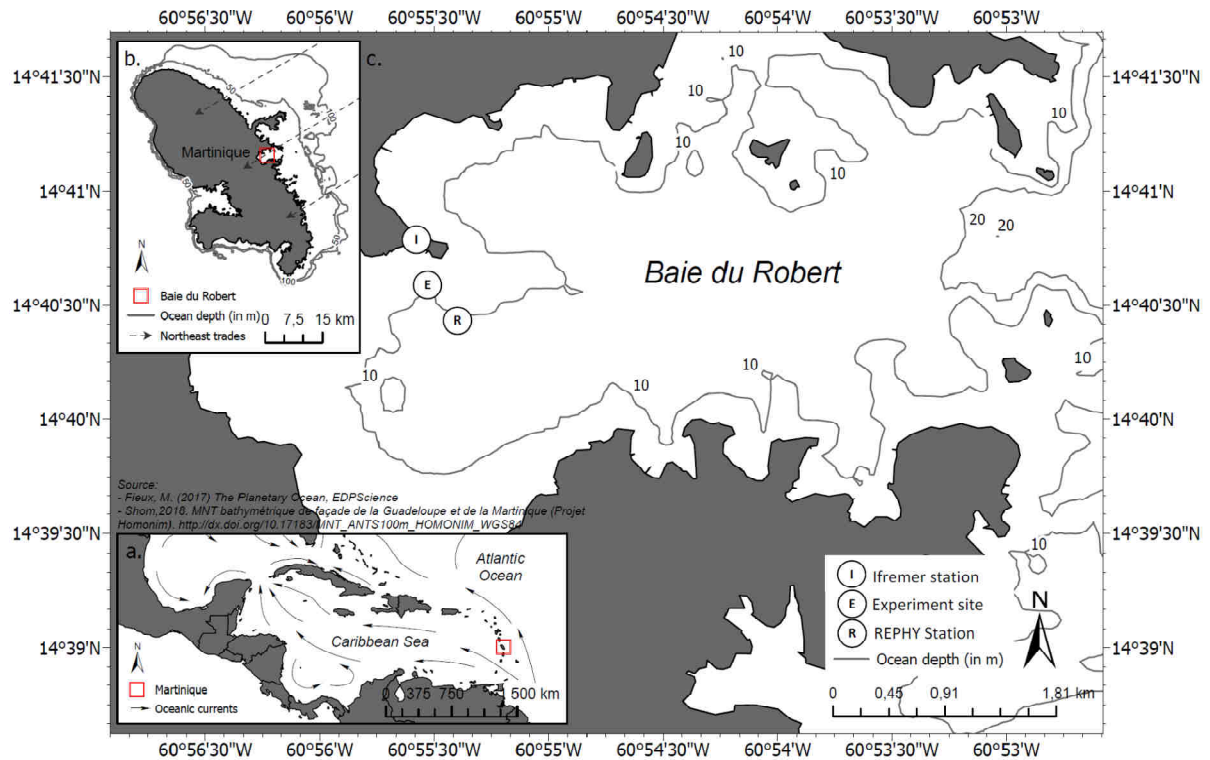


Fig. S1: Location of Ifremer station (I), experimental site (E) and REPHY monitoring station (R) with bathymetry. (a.) Regional position of Martinique Island, framed in red, with the main oceanic currents. (b.) Martinique Island with the orientation of the trade winds and location of Baie du Robert framed in red.

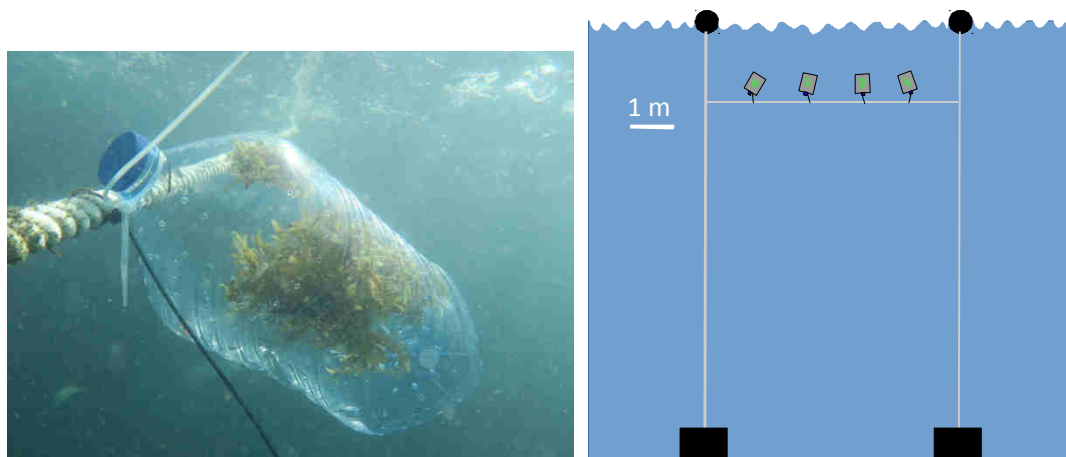


Fig. S2: Cultivation device: close-up picture of a 5 L bottles with its holes and *Sargassum* (left), arrangement of the bottles on the moorings (right).

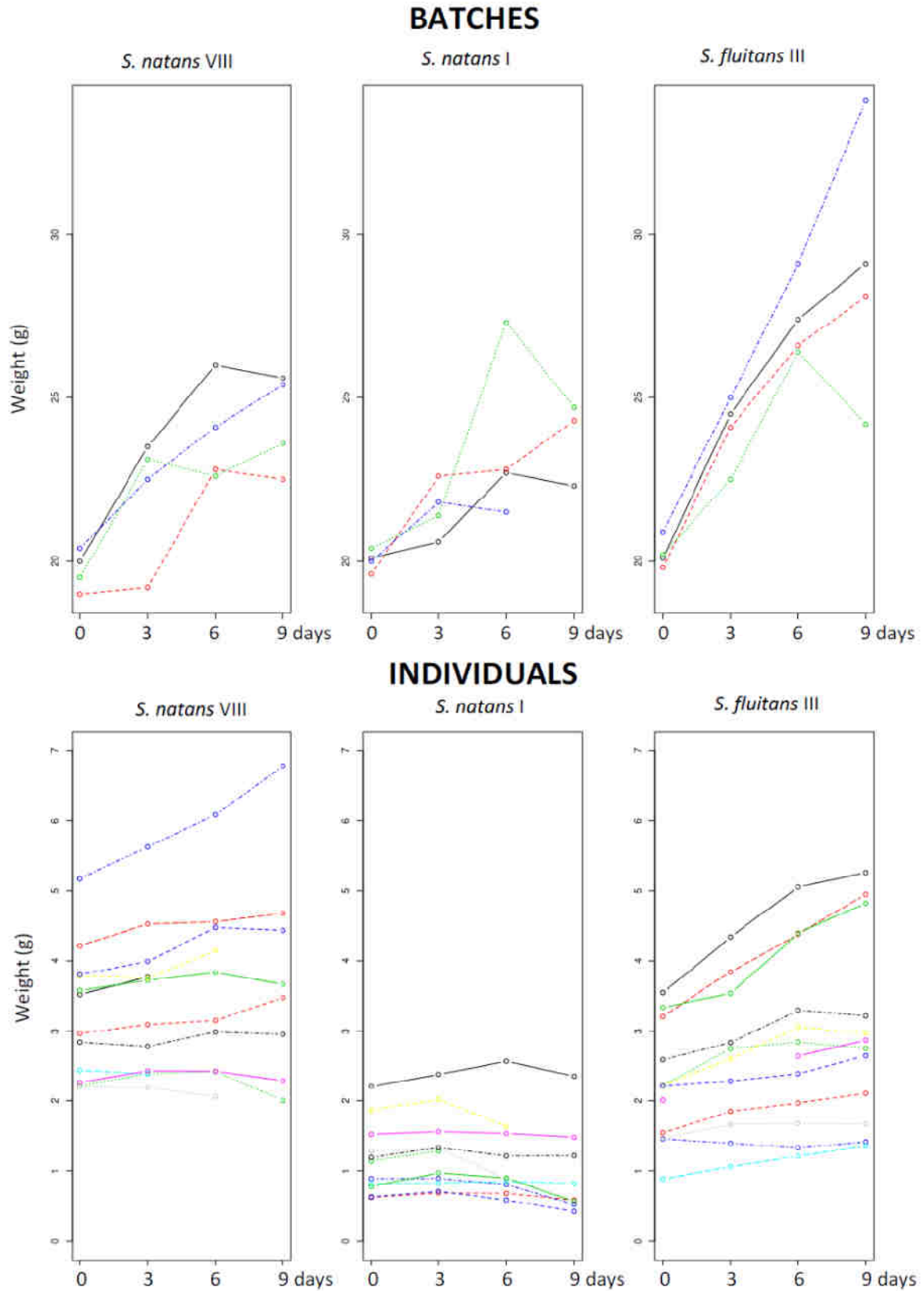


Fig. S3: *Sargassum* wet weight patterns of change over time for measurements of batches ($n = 4$) and individuals considering the different morphotypes (*S. natans* VIII ($n = 12$), *S. natans* I ($n = 12$), and *S. fluitans* III ($n = 12$)). Each line is a batch or an individual. It can be interrupted when a mark was lost or an apex dead or an individual broken in two parts.

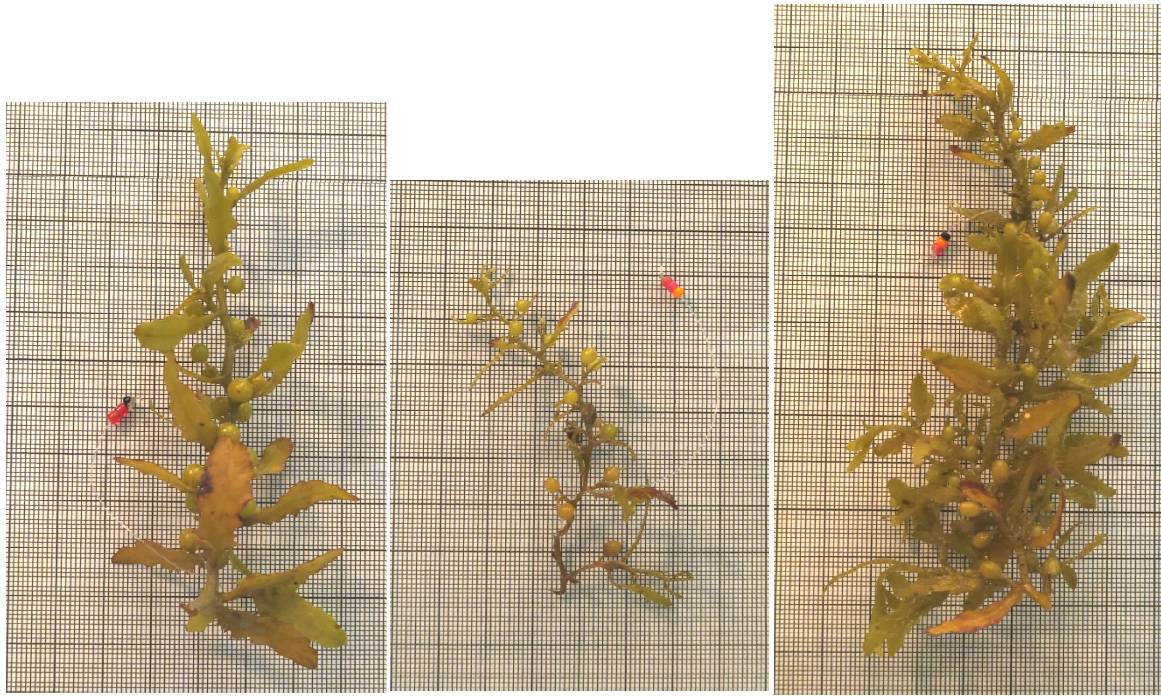


Fig. S4: *Sargassum* individuals after 9 days growth with *S. natans* VIII (left), *S. natans* I (middle), *S. fluitans* III (right) and their identification marks. The grid is 1 cm square.

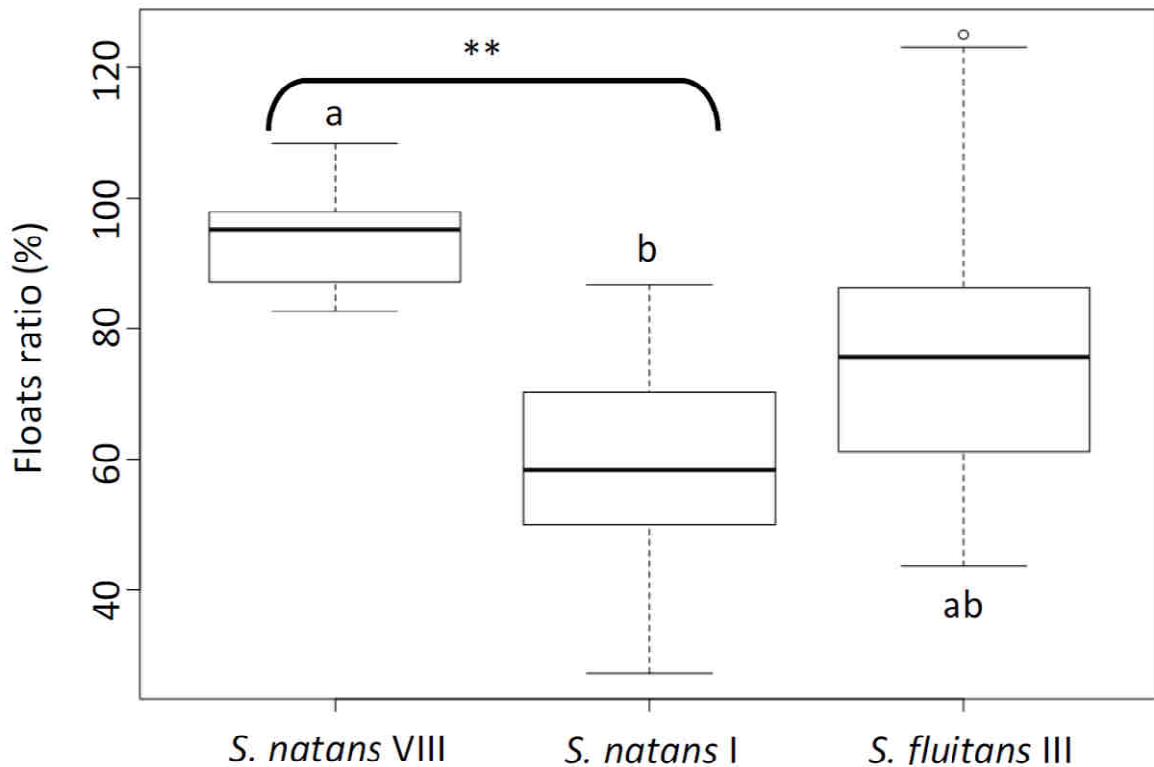


Fig. S5: Floats ratio after 9 days for the 3 morphotypes. Box shows the sample median and the first and third quartiles. Whiskers extend to the last data point which is no more than 1.5 times the interquartile range. Outliers are shown as dots. The KW test $\chi^2 = 10.76$, $df = 2$, $p\text{-value} = 0.004608$. The only significant Dunns post hoc test is between *S. natans* VIII vs *S. natans* I ($p = 0.00104^{**}$). Note

that some individuals *S. fluitans* III and *S. natans* VIII show values over 100% since they have more floats at the end of the experiment than at the beginning.

Table S1: Synthesis of Kruskal-Wallis and Dunns post hoc test results for the morphotype effect on *Sargassum* composition in %C, %N, %P, C:N, N:P, C:P, $\delta^{15}\text{N}$ (in ‰), $\delta^{13}\text{C}$ (in ‰).

	%C	%N	%P	C:N	N:P	C:P	$\delta^{13}\text{C}$	$\delta^{15}\text{N}$
Kruskal Wallis Chi2	3,62	6,635	5,235	10,955	1,28	0,335	11,115	11,185
df	2	2	2	2	2	2	2	2
p-value	0,164	0,036	0,073	0,004	0,527	0,846	0,004	0,004
Dunns p-value <i>S. natans</i> VIII vs <i>S. natans</i> I		0,022		0,005			0,671	0,179
Dunns p-value <i>S. natans</i> VIII vs <i>S. fluitans</i> III		0,031		0,003			0,002	0,048
Dunns p-value <i>S. natans</i> I vs <i>S. fluitans</i> III		0,888		0,888			0,008	0,001
Median	23,52%	1,14%	0,07%	23,85	30,33	827,43	-15,99	0,16
Median <i>S. natans</i> VIII		0,80%		35,86			-15,33	0,17
Median <i>S. natans</i> I		1,19%		22,03			-15,31	-0,38
Median <i>S. fluitans</i> III		1,20%		20,76			-16,75	1,33